Distributed Adaptive AC Droop Control in D-Q Coordinates for Inverter-Based Microgrids

Mehrzad Mohammadi Bijaieh[*], **Olugbenga Moses Anubi**[*†], **Charalambos Konstantinou**[*†]
[*]Center for Advanced Power Systems, Florida State University
[†]Department of Electrical and Computer Engineering, FAMU-FSU College of Engineering
E-mail: {mmohammadibijaieh, oanubi, ckonstantinou}@fsu.edu

***Abstract*—Droop control is a conventional method for operation of local distributed sources. Typical issues for droop control schemes include current sharing mismatch and voltage deviation, both likely to occur in a Microgrid (MG) setting. This paper proposes an adaptive droop scheme in d-q coordinates to compensate for current sharing mismatch at primary control level and voltage deviation compensation at secondary control. The droop resistances are adjusted for both d and q subsystems to eliminate the current sharing mismatch, and the droop voltage shifting method has been implemented to compensate for the voltage deviation. The dynamics of the proposed control is demonstrated for a three-phase reduced-order MG system using OpenModelica.**

***Index Terms*—Microgrids, droop control, distributed generation.**

I. Introduction

Microgrids are becoming more prevalent in distributed power generation [1]. Deployment of distributed energy sources (DERs) requires design and implementation of appropriate control systems. One of such schemes is droop control for dc [2], and ac systems [3]. In dc systems, droop control is implemented by creating virtual resistances between the generating sources [4]. Typically, in ac systems, the droop control is used to inject real power by deviating the frequency, and reactive power by changing the voltage amplitude.

In distributed control systems, for both ac and dc droop schemes, the power is subsequently shared between the sources by using local measurements and droop control settings. Local measurements may include voltages, currents, or both. Additionally, in ac systems, local synchronization can be achieved by utilization of Phase Locked Loops (PLLs) or Global Positioning System (GPS) [5], [6]. Droop settings, on the other hand, can be determined by a-priory and empirical knowledge as well as the mixture of both.

Hierarchical control for MG systems is proposed and widely used for ac and dc systems [7], [8]. In this case, the control system is divided into four main levels. At the lowest level of the hierarchy, a Device Level Controller (DLC) is used to ensure the stability and performance of the local system. This controller supports a primary controller which is typically a droop control scheme. It makes use of local measurements, low bandwidth communication and information from a higher secondary controller to provide local references to the DLC. At the distribution level, the secondary control aims to maintain the electrical levels of the MG and the synchronism of the Distributed Generation Units (DGUs) [9], [10]. At the highest level in the hierarchy, a tertiary controller manages energy production, optimization and energy trade with the grid or other MGs.

While droop control schemes are very effective for power sharing without communication networks, the lack of secondary loops might degrade the quality of electrical levels of the MG system. Specifically, the voltage at Point of Common Coupling (PCC) might suffer if the power demand from the load is significantly changed [4], or the accuracy of the power sharing might degrade when the values of the lines are not available [9], [11]. Hence, in order to ensure the appropriate power sharing and voltage regulation, it is of paramount importance to design additional control loops to dynamically change the droop settings.

The conventional ac droop control, or in short PQ droop control, is a well utilized scheme to share the active power by manipulating the frequency of operation. While this is a powerful method for distributed operation, it might not provide the best solution for fast inverter-based MGs where there is very little or no inertia [12].

In three-phase ac systems, d-q transformation is widely used to ease the analysis by replacing the stationary frame with a rotating frame to eventually transform the system into coupled dc sub-systems [13], [14]. MG reduced-order modeling based on d-q transformation is presented in [15], where dc control design and analysis have been leveraged for three-phase ac systems. d-q droop control is an alternative method for active and reactive power sharing without altering the system frequency. In this method, the control is implemented by employing the dc droop control for each d and q subsystems. The stability analysis is demonstrated in [12], and illustrative examples of performance in a hierarchical control approach are presented in [16], [17]. In [16], an external secondary controller solves a steady-state problem of the distribution system that handles the voltage regulation. Moreover, the current sharing operation depends on a single point of local voltage measurement. Here, an assumption is that the exact values of the lines and loads are available which is a major simplification for initial stages of control system design. In MGs, it is most likely that the exact values of the system components are unknown. Therefore, the design of a compensatory control system is appropriate.

In this paper, an adaptive droop scheme in d-q coordinates for MGs with topologies such as Fig. 1 is proposed. At the primary level, the droop resistances are tuned using a Proportional and Integral (PI) controller that aims to remove the current sharing inaccuracies. Additionally, an adaptive secondary controller based on curve shifting method is used to alleviate the bus voltage drop. In this work, the focus is on secondary and primary control levels; hence, DLCs and tertiary controllers are not discussed and they are left for future iterations.

This paper is organized as follows. First, the overall reduced-order state-space model of the microgrid system is presented. Then, the basic and the proposed adaptive droop control are introduced. Finally, the performance of the proposed control is demonstrated using OpenModelica [18].

II. Microgrid Model in d-q Coordinates

The overall reduced-order microgrid model, adopted from [15], is demonstrated in Fig. 1. This topological representation of the three-phase MG system includes parallel DGUs (indexed by i), transmission/filter RL lines, a common bus (represented by v_{db} and v_{qb} corresponding to d and q coordinates) and an RLC load. The state-space model of the system under balanced conditions is:

$$L_{line,i}\frac{di_{d,i}}{dt} = -Ri_{d,i} + \omega L_{line,i}i_{q,i} + v_{s,d,i} - v_{db} \tag{1a}$$
$$L_{line,i}\frac{di_{q,i}}{dt} = -Ri_{q,i} - \omega L_{line,i}i_{d,i} + v_{s,q,i} - v_{qb} \tag{1b}$$
$$C_b\frac{dv_{db}}{dt} = i_{db} + \omega C_b v_{qb} - i_{dLb} \tag{1c}$$
$$C_b\frac{dv_{qb}}{dt} = i_{qb} - \omega C_b v_{db} - i_{qLb} \tag{1d}$$
$$L_b\frac{di_{dLb}}{dt} = -R_b i_{dLb} + \omega L_b i_{qLb} + v_{db} \tag{1e}$$
$$L_b\frac{di_{qLb}}{dt} = -R_b i_{qLb} - \omega L_b i_{dLb} + v_{qb}, \tag{1f}$$

where,

$$i_{db} = \sum_{i=1}^{n} i_{d,i}, \quad and \quad i_{qb} = \sum_{i=1}^{n} i_{q,i}. \tag{2}$$

In (1) and (2), $i = 0...N$, where N represents the number of parallel DGUs. The first two expressions of (1) include the local systems with the corresponding RL lines. Here, the control variables are $v_{s,d,i}$ and $v_{s,q,i}$ which represent the three-phase output voltages of inverters [15], [17]. In the next sections, the control system will be designed to control these voltages using the adaptive d-q droop control scheme.

III. Droop Control in d-q Coordinates

The overall control scheme is shown in Fig. 2. Considering the curve shifting method in Fig. 3, the d-q droop control with one local current measurement is:

$$v_{d,ref,i} = v_{d,ref} - r_{d,i}i_{d,i} \tag{3a}$$
$$v_{q,ref,i} = v_{q,ref} - r_{q,i}i_{q,i}, \tag{3b}$$

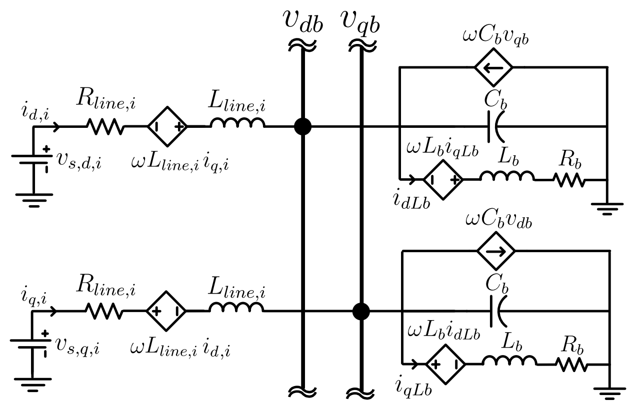

Fig. 1. MG model in d-q coordinates for parallel DGUs with corresponding RL lines and an RLC load.

where $i_{d,i}$ and $i_{q,i}$ represent the measured currents, $v_{d,ref}$ and $v_{q,ref}$ denote the reference voltages at no load, $r_{d,i}$ and $r_{q,i}$ are the droop resistances, and $v_{d,ref,i}$ and $v_{q,ref,i}$ are the individual voltage commands in d and q coordinates, respectively.

For a typical droop scheme, considering Fig. 3, for specific $v_{d,ref}$ and $v_{q,ref}$ values, the actual bus voltage settled values are denoted by v_{db} and v_{qb}. As the load values change, this voltage might not match the nominal value represented by v^*_{db} and v^*_{qb}. Hence, $v_{d,ref}$ and $v_{q,ref}$ can be dynamically changed so that the settling value matches the nominal bus voltage. Moreover, $r_{d,i}$ and $r_{q,i}$ can be tuned to maintain the rated currents. In the next section, the adaptive droop with such approach is presented.

IV. Adaptive Droop Control in d-q Coordinates

The proposed adaptive droop control is:

$$v_{d,ref,i} = v_{d,ref} - (r_{d,i,init} + \delta R_{d,i})i_{d,i} + \Delta v_{db} \tag{4a}$$
$$v_{q,ref,i} = v_{q,ref} - (r_{q,i,init} + \delta R_{q,i})i_{q,i} + \Delta v_{qb}, \tag{4b}$$

where Δv_{db} and Δv_{qb} are the voltage deviation commands obtained from the secondary control, $\delta R_{d,i}$ and $\delta R_{q,i}$ denote the droop resistance changes, and $r_{d,i,init}$ and $r_{q,i,init}$ are the initial guesses for the resistance values. In the secondary loop, voltage deviation commands are obtained from:

$$\Delta v_{db} = K_{d,p,v}(t)e_{d,v}(t) + K_{d,i,v}(t)\int_0^{\tau} e_{d,v}(\tau)d\tau \tag{5a}$$
$$\Delta v_{qb} = K_{q,p,v}(t)e_{q,v}(t) + K_{q,i,v}(t)\int_0^{\tau} e_{q,v}(\tau)d\tau, \tag{5b}$$

where $K_{d,p,v}$, $K_{q,p,v}$, $K_{d,i,v}$, and $K_{q,i,v}$ represent the PI gains for d and q sub-systems. In the above expressions, $e_{d,v}$ and $e_{q,v}$ are obtained from:

$$e_{d,v} = v^*_{db} - v_{db} \tag{6a}$$
$$e_{q,v} = v^*_{qb} - v_{qb}, \tag{6b}$$

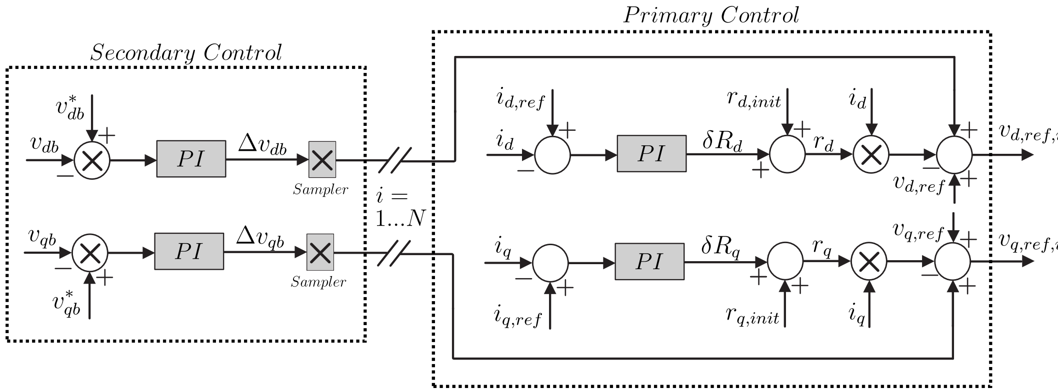

Fig. 2. The proposed adaptive droop control in d-q coordinates.

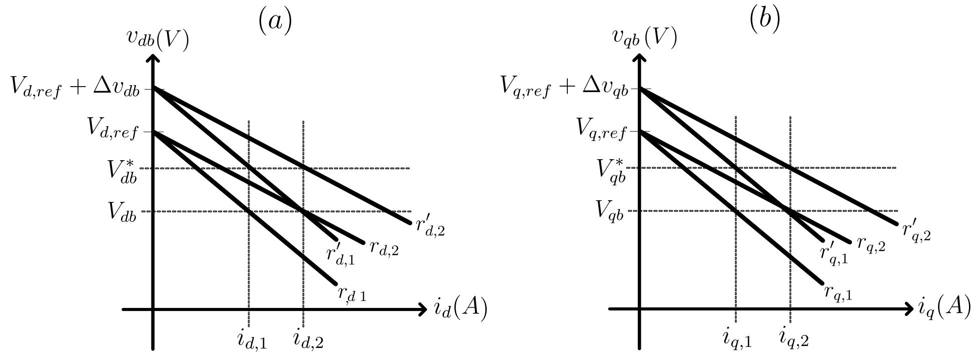

Fig. 3. Adaptive droop control in d and q coordinates.

where v_{db} and v_{qb} are the measured bus voltages, and v_{db}^* and v_{qb}^* are the corresponding nominal values. In (4), if the overall droop resistances, $r_{d,i}$ and $r_{q,i}$ are defined as:

$$r_{d,i} = \delta R_{d,i} + r_{d,i,init} \tag{7a}$$

$$r_{q,i} = \delta R_{q,i} + r_{q,i,init}, \tag{7b}$$

$\delta R_{d,i}$ and $\delta R_{q,i}$ can be set as:

$$\delta R_{d,i} = K_{d,p,i}(t) e_{d,i}(t) + K_{d,i,i}(t) \int_0^{\tau} e_{d,i}(\tau) d\tau \tag{8a}$$

$$\delta R_{q,i} = K_{q,p,i}(t) e_{q,i}(t) + K_{q,i,i}(t) \int_0^{\tau} e_{q,i}(\tau) d\tau. \tag{8b}$$

where $K_{d,p,i}$, $K_{q,p,i}$, $K_{d,i,i}$, and $K_{q,i,i}$ represent the PI gains for d and q sub-systems. In this expression, $e_{d,i}$ and $e_{q,i}$ are obtained from:

$$e_{d,i} = i_{d,i} - i_{ref,d,i} \tag{9a}$$

$$e_{q,i} = i_{q,i} - i_{ref,q,i}, \tag{9b}$$

where $i_{d,i}$ and $i_{q,i}$ are the measured current components. In (9), $i_{ref,d,i}$ and $i_{ref,q,i}$ can be obtained from:

$$I_{ref,d,i} = \gamma_i i_{db} \tag{10a}$$

$$I_{ref,q,i} = \gamma_i i_{qb}, \tag{10b}$$

where i_{db} and i_{qb} are the load currents. γ_i is the indexed weighting parameter for individual converters and should meet $\sum_{i=1}^{N} \gamma_i = 1$.

The load currents in (10) as well as the bus voltage measurements in (6) are used by the secondary controller. The outputs are eventually used by the droop control, and the resistances in (8) are adaptively tuned in order to remove the error between the locally measured currents and the corresponding desired values. It is important to note that the secondary control loop operates at a lower bandwidth compared to the droop control loop. Hence, the sampling rate of Δv_{db} and Δv_{qb} is lower than $\delta R_{d,i}$ and $\delta R_{q,i}$.

TABLE I
LOAD STEP CASE MG PARAMETERS

DGU Line Parameters		
	$R_{line}(\Omega)$	$L_{line}(mH)$
TR-Line 1	0.6	1.6
TR-Line 2	0.5	1.1
RC Load Parameters		
	$L(mH)$	$C(\mu F)$
Load	0.001	86

V. SIMULATION

The two DGU system of Fig. 1 ($N = 2$), with parameter values in Table I, is simulated in OpenModelica simulation package. The aim is to step the load and observe the adaptive behavior of the control system to maintain the load bus at 120 V_{rms} and keep the current sharing when $\gamma_1 = 0.4$ and $\gamma_2 = 0.6$. In this case, the currents, and subsequently the powers injected by DGU 2 are maintained to be 50% more than of DGU 1. The corresponding results are shown in Figs. 4 to 8. The control network update-rate may affect the performance and stability of the overall system and should be

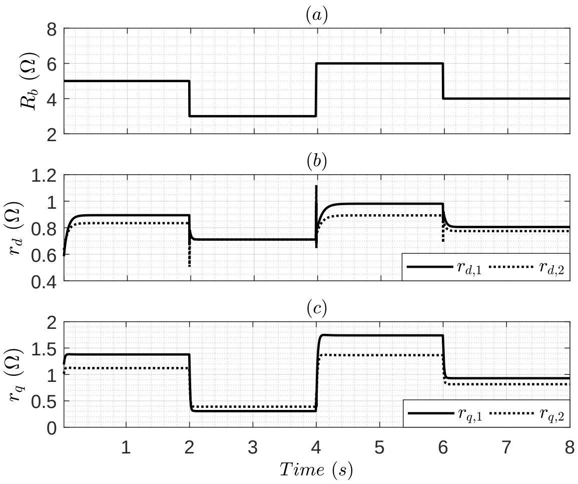

Fig. 4. (a) Load resistance step changes at $t = 2s$, $4s$ and $6s$. The corresponding DGU 1 and DGU 2 adaptive droop resistances for (b) d, and (c) q subsystems.

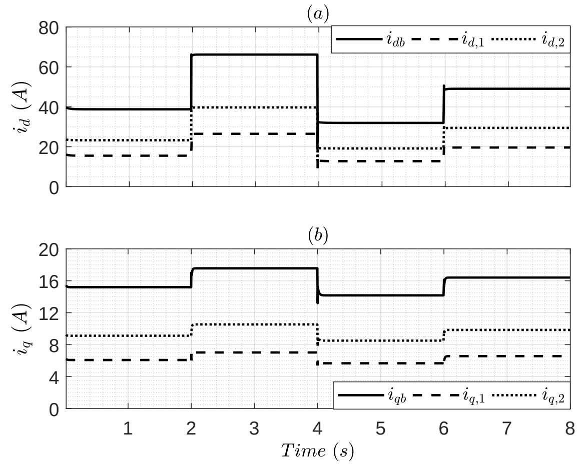

Fig. 5. Overall load current and the corresponding individual DGU current shares for (a) d, and (b) q subsystems.

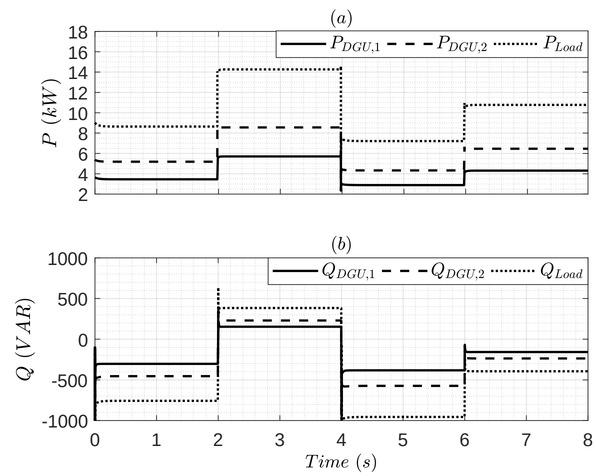

Fig. 6. Overall individual and load (a) active, and (b) reactive powers for DGU 1 and DGU 2.

chosen carefully [16]. Here, for the secondary control level operation, the load currents in (10) and the load bus voltages in (6) are measured at the rate of $8\ ms$. It is important to note that for field deployed MG systems the robustness of the controller against various uncertainty should be guaranteed. Here, the component values and the control parameters are chosen to serve the control system for illustrative purposes and design, implementation, and practical verification of high fidelity models with appropriate filtering are left for future work.

Fig. 4a demonstrates the load step changes throughout a simulation of $8s$. Figs. 4b and 4c show the adapted droop resistance values for the two DGUs for each d and q subsystems. It can be seen that the droop resistances are adjusted versus the load change to effectively maintain the current sharing of $0.4 : 0.6$. The overall load current and individually shared i_d and i_q components are shown in Fig. 5. The overall active and reactive load power as well as individual DGU power sharing are shown in Fig. 6. It can be seen that the sharing ratio of $0.4 : 0.6$ for active and reactive power injections is effectively maintained versus load variations.

It is important to note that the dynamics of droop resistance deviations depend on the gains of the PI controllers in (8). For this simulation case, the gains are $K_{d,p,1} = K_{d,p,2} = 0.02$, $K_{q,d,1} = K_{q,d,2} = 0.1$ and $K_{d,i,1} = K_{d,i,2} = 10$, $K_{q,i,1} = K_{q,i,2} = 100$ for the proportional and integral compensatory controllers in d and q coordinates. The choice of these gains can significantly affect the response as well as the stability of the overall system. In this work, these gains are chosen arbitrarily and in a conservative manner with stability taking precedence. However, they can be dynamically changed versus the large variations of load and system setpoints so that a desired trade-off between stability and response time is achieved [19].

Fig. 7 shows individual d-q droop control commands that are obtained from (4). Figs. 8a and 8b demonstrate the maintained load bus d-q voltages and Fig. 8c shows the three-phase voltages around $t = 4\ s$. It can be seen that the secondary controller effectively shifts the droop curve to compensate for bus voltage mismatch. It is evident that the overall control system effectively maintains the peak value of $170\ V$ equivalent to $208\ V_{l-l}$ or $120\ V_{rms}$ while satisfying both active and reactive power sharing.

VI. Summary and Conclusions

In this paper, an adaptive droop control is proposed to maintain the load bus voltage and the current sharing accuracy of parallel inverter-based three-phase MGs in d-q coordinates. The two adaptive sets of PI control loops include a secondary and a primary control level. The secondary control is defined to compensate for voltage deviation at the load bus by using a single point of voltage measurement. And the droop control, as the primary controller, is modified to ensure the current sharing accuracy. It is shown that the droop virtual resistances can be dynamically modified versus load changes so that the current sharing accuracy is maintained. The droop voltage shifting

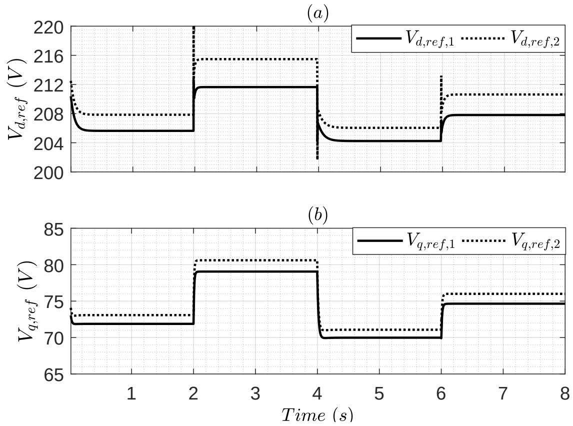

Fig. 7. Adaptive control of two DGU droop voltage settings in (a) d, and (b) q coordinates.

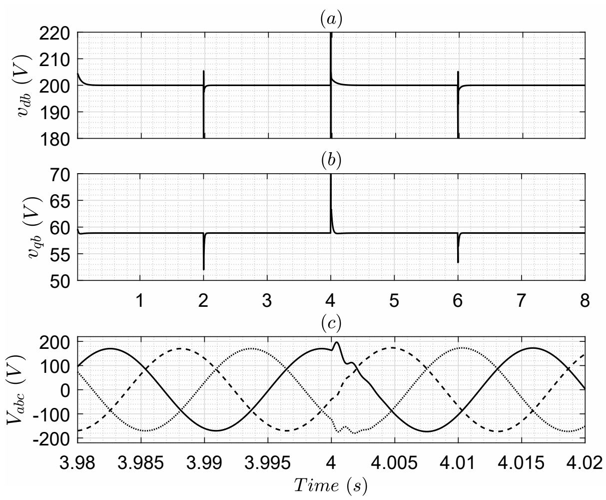

Fig. 8. The maintained load voltage for (a) d, and (b) q subsystems. (c) the three-phase voltages when the load steps from 3Ω to 6Ω at $t = 4s$.

method can be used to match a nominal value of the load bus voltage. The behavior of the system under the proposed control is demonstrated for two parallel DGUs sharing active and reactive powers to support a three-phase RLC load.

VII. Future Work

A more detailed hierarchical controller will be employed to study the MG system under the proposed control. For example, the overall control commands, $v_{d,ref,i}$ and $v_{q,ref,i}$ in (4), could be fed into a variety of local DLCs such as sliding mode or PI controllers [20]. Also, alternative compensatory methods such as model predictive control will be investigated. Additionally, a comprehensive stability analysis of the overall control system will be performed to define the thresholds and obtain the criteria for control parameters such as primary and secondary PI gains. Further on, the cyber-physical nature of the presented concepts will be addressed to further study the control system components and parameters for design purposes. Specifically, the effects of rotating frame synchronization and sensor measurement perturbations on stability criteria will be investigated.

References

[1] B. Lasseter, "Microgrids [distributed power generation]," *Proceedings IEEE Power Engineering Society Winter Meeting,*, vol. 1, pp. 146–149, Jan. 2001.

[2] B. K. Johnson, R. H. Lasseter, F. L. Alvarado, and R. Adapa, "Expandable multiterminal dc systems based on voltage droop," *IEEE Transactions on Power Delivery*, vol. 8, no. 4, pp. 1926–1932, 1993.

[3] A. Tuladhar, H. Jin, T. Unger, and K. Mauch, "Parallel operation of single phase inverter modules with no control interconnections," *Proceedings IEEE APEC*, pp. 94–100, 1997.

[4] W. W. Weaver, R. D. Robinett, G. G. Parker, and D. G. Wilson, "Distributed control and energy storage requirements of networked dc microgrids," *Control Engineering Practice*, vol. 44, pp. 10 – 19, 2015.

[5] M. S. Golsorkhi, D. D. C. Lu, and J. M. Guerrero, "A gps-based decentralized control method for islanded microgrids," *IEEE Transactions on Power Electronics*, vol. 32, pp. 1615–1625, Feb. 2017.

[6] A. H. Etemadi, E. J. Davison, and R. Iravani, "A decentralized robust control strategy for multi-der microgrids: Part I-fundamental concepts," *IEEE Transactions on Power Delivery*, vol. 27, no. 4, pp. 1843–1853, 2012.

[7] J. M. Guerrero, J. C. Vasquez, J. Matas, L. G. de Vicuna, and M. Castilla, "Hierarchical control of droop-controlled ac and dc microgrids- a general approach toward standardization," *IEEE Transactions on Industrial Electronics*, vol. 58, pp. 158–172, Jan 2011.

[8] C. Jin, P. Wang, J. Xiao, Y. Tang, and F. H. Choo, "Implementation of hierarchical control in dc microgrids," *IEEE Transactions on Industrial Electronics*, vol. 61, pp. 4032–4042, Aug 2014.

[9] V. Nasirian, A. Davoudi, F. L. Lewis, and J. M. Guerrero, "Distributed adaptive droop control for dc distribution systems," *IEEE Transactions on Energy Conversion*, vol. 29, pp. 944–956, Dec 2014.

[10] Q. Shafiee, J. C. Vasquez, J. M. Guerrero, V. Nasirian, and A. Davoudi, "Cooperative frequency control for autonomous ac microgrids," in *2015 IEEE Eindhoven PowerTech*, pp. 1–6, June 2015.

[11] W. Yao, M. Chen, J. Matas, J. M. Guerrero, and Z. Qian, "Design and analysis of the droop control method for parallel inverters considering the impact of the complex impedance on the power sharing," *IEEE Transactions on Industrial Electronics*, vol. 58, pp. 576–588, Feb 2011.

[12] M. Toub, M. M. Bijaieh, W. W. Weaver, R. D. R. III, M. Maaroufi, and G. Aniba, "Droop control in dq coordinates for fixed frequency inverter-based ac microgrids," *Electronics*, vol. 8, no. 10, 2019.

[13] W. C. Duesterhoeft, M. W. Schulz, and E. Clarke, "Determination of instantaneous currents and voltages by means of alpha, beta, and zero components," *Transactions of the American Institute of Electrical Engineers*, vol. 70, pp. 1248–1255, July 1951.

[14] T. A. Lipo, "A cartesian vector approach to reference theory of ac machines," in *Int. Conference On Electric Machines*, Sep 1984.

[15] T. Hassell, W. W. Weaver, R. D. Robinett, D. G. Wilson, and G. G. Parker, "Modeling of inverter based ac microgrids for control development," *2015 IEEE Conference on Control Applications (CCA)*, pp. 1347–1353, 2015.

[16] M. Mohammadi Bijaieh, W. Weaver, and R. D. Robinett III, "Energy storage requirements for inverter-based microgrids under droop control in d-q coordinates," *IEEE Transactions on Energy Conversion*, pp. 1–10, 2019.

[17] M. M. Bijaieh, W. W. Weaver, and R. D. Robinett, "Effects of dq droop settings on energy storage systems of inverter-based microgrids," in *2018 International Symposium on Power Electronics, Electrical Drives, Automation and Motion (SPEEDAM)*, pp. 75–80, June 2018.

[18] P. Fritzson, *Principles of Object-Oriented Modeling and Simulation with Modelica 3.3: A Cyber-Physical Approach*. Wiley-IEEE Press, 2 ed., Apr. 2015.

[19] M. Mokhtar, M. I. Marei, and A. A. El-Sattar, "An adaptive droop control scheme for dc microgrids integrating sliding mode voltage and current controlled boost converters," *IEEE Transactions on Smart Grid*, vol. 10, pp. 1685–1693, March 2019.

[20] A. Arzani, P. Arunagirinathan, and G. K. Venayagamoorthy, "Development of optimal pi controllers for a grid-tied photovoltaic inverter," in *2015 IEEE Symposium Series on Computational Intelligence*, pp. 1272–1279, Dec 2015.